J|A|C|S
ARTICLES
Published on Web 04/05/2002

A Novel Isomerization on Interaction of Antitumor-Active Azole-Bridged Dinuclear Platinum(II) Complexes with 9-Ethylguanine. Platinum(II) Atom Migration from N2 to N3 on 1,2,3-Triazole

Seiji Komeda,[†] Martin Lutz,[‡] Anthony L. Spek,[‡] Yasuyuki Yamanaka,[§] Takaji Sato,[§] Masahiko Chikuma,[§] and Jan Reedijk*,[†]

Contribution from the Leiden Institute of Chemistry, Gorlaeus Laboratories, Leiden University, P.O. Box 9502, 2300 RA Leiden, The Netherlands, Department of Crystal & Structural Chemistry, Bijvoet Center for Biomolecular Research, Utrecht University, Padualaan 8, 3584 CH Utrecht, The Netherlands, and Osaka University of Pharamaceutical Sciences, 4-20-1 Nasahara, Takatsuki 569-1094, Japan

Received August 16, 2001

Abstract: The reactions of the dinuclear platinum(II) complexes, [{*cis*-Pt(NH_3)$_2$}$_2$(μ-OH)(μ-pz)](NO_3)$_2$ (**1**, pz = pyrazolate), [{*cis*-Pt(NH_3)$_2$}$_2$(μ-OH)(μ-1,2,3-ta-*N1,N2*)](NO_3)$_2$ (**2**, 1,2,3-ta = 1,2,3-triazolate), and a newly prepared [{*cis*-Pt(NH_3)$_2$}$_2$(μ-OH)(μ-4-phe-1,2,3-ta-*N1,N2*)](NO_3)$_2$ (**3**, 4-phe-1,2,3-ta = 4-phenyl-1,2,3-triazolate), whose crystal structure was determined, with 9-ethylguanine (9EtG) have been monitored in aqueous solution at 310 K by means of ^{1}H NMR spectroscopy. The dinuclear platinum(II) complexes **1**−**3** each react with 9EtG in a bifunctional way to form 1:2 complexes, [{*cis*-Pt(NH_3)$_2$(9EtG-*N7*)}$_2$(μ-pz)]$^{3+}$ (**4**), [{*cis*-Pt(NH_3)$_2$(9EtG-*N7*)}$_2$(μ-1,2,3-ta-*N1,N3*)]$^{3+}$ (**5**), and [{*cis*-Pt(NH_3)$_2$(9EtG-*N7*)}$_2$(μ-4-phe-1,2,3-ta-*N1,N3*)]$^{3+}$ (**6**). The reactions of **2** and **3** involve a novel isomerization, in which the Pt atom, initially bound to N2 on the 1,2,3-ta, migrates to N3 after the first substitution by N7 of 9EtG. This isomerization reaction has been unambiguously characterized by 1D and 2D NMR spectroscopy and pH titration. The reactions of **2** and **3** with 9EtG show faster kinetics, and the second-order rate constants (k) for the reactions of **1**−**3** are 1.57×10^{-4}, 2.53×10^{-4}, and 2.56×10^{-4} M^{-1} s^{-1}, respectively. The pK_a values at the N1H site of 9EtG were determined for **4**−**6** from the pH titration curves. Cytotoxicity assays of **1**−**3** were performed in L1210 murine leukemia cell lines, respectively sensitive and resistant to cisplatin. In the parent cell line, **2** and **3** exhibit higher cytotoxicity compared to cisplatin, especially, **2** is 10 times as active as cisplatin. **1** was found to be less cytotoxic than cisplatin, but still in the active range and more active than cisplatin in a cisplatin-resistant cell line.

Introduction

Cisplatin is one of the most widely utilized anticancer agents, and is effective especially in clinical treatment of testicular and ovarian cancers.[1−3] However, some of the clinical inconveniences still remain, such as acquired drug resistance and serious side effects.[4,5] These inconveniences are a great challenge to circumvent. In addition, the applicability of cisplatin is still limited to a relatively narrow range of tumors. The main target of cisplatin is generally accepted to be DNA, especially the configuration of the major intrastrand cross-link at the GpG site is likely to be responsible for the antitumor activity.[6,7] The DNA in this adduct is severely distorted from normal B DNA, and the duplex is bent by 40−80° toward the major groove as determined by a variety of methods.[8−11] Therefore, and to overcome intrinsic and acquired resistance, a rational approach would be to prepare platinum complexes that react with DNA in mechanisms distinct from cisplatin and its analogues. Some classes of platinum(II) complexes with two or three platinum-amine units linked by a variable-length diamine chain have already been shown to be successful approaches lacking cross-resistance.[12−14] These complexes serve as novel types of intra-

* Address correspondence to this author. E-mail: reedijk@chem.Leidenuniv.nl.
[†] Leiden University.
[‡] Utrecht University.
[§] Osaka University of Pharamaceutical Sciences.

(1) (a) Rosenberg, B.; Van Camp, L.; Krigas, T. *Nature* **1965**, *205*, 698. (b) Rosenberg, B.; Van Camp, L.; Trosko, J. E.; Mansour, V. H. *Nature* **1969**, *222*, 385.
(2) Jamieson, E. R.; Lippard, S. J. *Chem. Rev.* **1999**, *99*, 2467.
(3) (a) Reedijk, J. *Chem. Commun.*, **1996**, 801. (b) Reedijk, J. *Chem. Rev.* **1999**, *94*, 2699.
(4) Burchenal, J. H.; Kalaher, K.; Dew, K.; Lokys, L.; Gale, G. *Biochimie* **1978**, *60*, 961.
(5) Eastman, A.; Bresnick, E. *Biochem. Pharmacol.* **1981**, *30*, 2721.
(6) Fichtinger-Schepman, A. M. J.; van der Veer, J. L.; den Hartog, J. H. J.; Lohman, P. H. M.; Reedijk, J. *Biochemistry* **1985**, *24*, 707.
(7) Pil, P. M.; Lippard, S. J. *Science* **1992**, *256*, 234.
(8) Yang, D.; Van Boom, S. S. G. E.; Reedijk, J.; Van Boom, J. H.; Wang, A. H.-J. *Biochemistry* **1995**, *34*, 12912.
(9) Gelasco, A.; Lippard, S. J. *Biochemistry* **1998**, *37*, 9230.
(10) Takahara, P. M.; Rosenzweig, A. C.; Frederick, C. A.; Lippard, S. J. *Nature* **1995**, *377*, 649.
(11) Marzilli, L. G.; Saad, J. S.; Kuklenyik, Z.; Keating, K. A.; Xu, Y. H. *J. Am. Chem. Soc.* **2001**, *123*, 2764.
(12) Qu, Y.; Farrell, N. *J. Am. Chem. Soc.* **1991**, *113*, 4851.

10.1021/ja0168559 CCC: $22.00

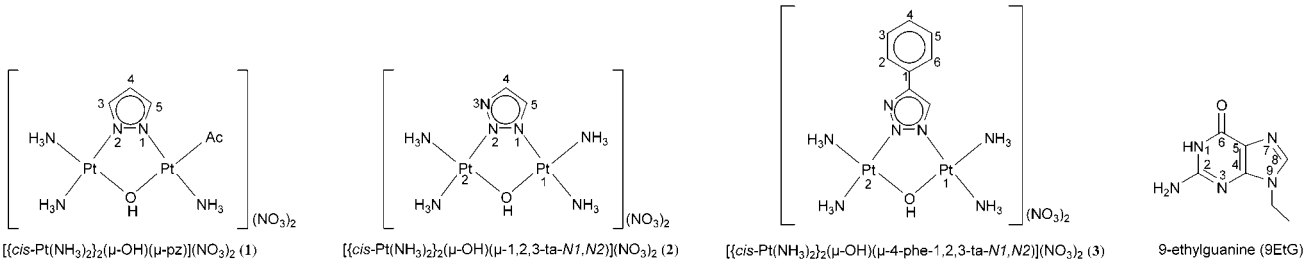

Figure 1. Schematic representation of [{*cis*-Pt(NH$_3$)$_2$}$_2$(μ-OH)(μ-pz)](NO$_3$)$_2$ (**1**), [{*cis*-Pt(NH$_3$)$_2$}$_2$(μ-OH)(μ-1,2,3-ta-*N1,N2*)](NO$_3$)$_2$ (**2**), [{*cis*-Pt(NH$_3$)$_2$}$_2$-(μ-OH)(μ-4-phe-1,2,3-ta-*N1,N2*)](NO$_3$)$_2$ (**3**), and 9-ethylguanine (9EtG).

and interstrand cross-links,[15] suggesting that different DNA-binding modes indeed may have different biological effects. Recently highly cytotoxic azole-bridged dinuclear platinum(II) complexes were introduced by some of us.[16,17] Two of these, e.g. the compounds, [{*cis*-Pt(NH$_3$)$_2$}$_2$(μ-OH)(μ-pz)](NO$_3$)$_2$ (**1**, pz = pyrazolate) and [{*cis*-Pt(NH$_3$)$_2$}$_2$(μ-OH)(μ-1,2,3-ta-*N1,N2*)](NO$_3$)$_2$ (**2**, 1,2,3-ta = 1,2,3-triazolate), exhibit significantly higher cytotoxicity than cisplatin on several human tumor cell lines. The purpose of this class of dinuclear platinum(II) complexes is to provide a 1,2-intrastrand cross-link with minimal kink of DNA, which would trigger the desired cytotoxic effects.[16−18] The complexes possess two platinum centers bridged by azolato and hydroxo anions; the OH$^-$ acts as a leaving group to provide a bifunctional coordination on DNA. The geometry of the crystal structure of [{*cis*-Pt(NH$_3$)$_2$-(9EtG-*N7*)}$_2$(μ-pz)]$^{3+}$ cation has confirmed that **1** may indeed provide 1,2-intrastrand GG cross-links with less local distortions upon binding DNA, compared to cisplatin.[16] For complex **2**, however, the reaction mechanism with nucleobases or nucleic acids has not been studied yet. It is of great interest whether the platinum atom bound to N2 of the 1,2,3-ta ring can remain in the present position after the substitution of the hydroxide group for nucleic acid. Accordingly, migration from N2 to N3 of the platinum atom should be considered. For comparison, another dinuclear platinum(II) complex, [{*cis*-Pt(NH$_3$)$_2$}$_2$(μ-OH)(μ-4-phe-1,2,3-ta-*N1,N2*)](NO$_3$)$_2$ (**3**, 4-phe-1,2,3-ta = 4-phenyl-1,2,3-triazolate) was newly prepared. This paper describes the crystal structure of **3**, kinetics and mechanisms of all three antitumor-active dinuclear platinum(II) complexes upon reaction with nucleobase, as well as a cytotoxic study with a cisplatin-resistant cell line. A unique and novel isomerization is observed, where Pt(II) migrates from N2 to N3 in the triazole ring, upon reaction with the guanine-N7 site.

Experimental Section

Materials. 9-Ethylguanine (9EtG) and K_2PtCl_4 were obtained from Sigma and Johnson & Matthey (Reading, UK), respectively. The starting materials, [*cis*-Pt(NH$_3$)$_2$(μ-OH)]$_2$(NO$_3$)$_2$[19] and *1H*-4-phenyl-1,2,3-triazole,[20] were prepared according to the literature method. The azole-bridged dinuclear platinum(II) complexes, [{*cis*-Pt(NH$_3$)$_2$}$_2$(μ-OH)(μ-pz)](NO$_3$)$_2$ (**1**), [{*cis*-Pt(NH$_3$)$_2$}$_2$(μ-OH)(μ-1,2,3-ta-*N1,N2*)](NO$_3$)$_2$ (**2**), and [{*cis*-Pt(NH$_3$)$_2$(9EtG-*N7*)}$_2$(μ-OH)(μ-pz)](NO$_3$)$_3$ (**4**), were synthesized according to the published methods.[16,17]

Preparation of [{*cis*-Pt(NH$_3$)$_2$}$_2$(μ-OH)(μ-4-phe-1,2,3-ta-*N1,N2*)](NO$_3$)$_2$ (3). A σ-ligand metathesis reaction with concomitant release of a water molecule[16,17,21] was applied for the synthesis of **3**. *1H*-4-phe-1,2,3-Hta (0.353 g, 2.43 mmol) was added to a solution of 0.5 g of [*cis*-Pt(NH$_3$)$_2$(μ-OH)]$_2$(NO$_3$)$_2$ (0.81 mmol) in 50 mL of water. The solution was stirred and heated at 60 °C for 4 h in the dark, and was then filtered and evaporated to dryness. The resulting white material was washed with 200 mL of ice-cold EtOH and diethyl ether. Recrystallization was carried out from water.

Yield: 0.25 g (42%). Anal. Calcd for $C_8H_{19}N_9O_7Pt_2$: C, 12.92; H, 2.58; N, 16.96. Found: C, 12.84; H, 2.44; N, 17.11. ^{1}H NMR (D$_2$O): δ (4-phe-1,2,3-ta resonance) 8.01 (1H, s, ta(5)), 7.82 (2H, d, phe(2,6)), 7.55 (2H, t, phe(3,5)), 7.50 (1H, t, phe(4)). ^{195}Pt NMR (D$_2$O): δ −2098, −2149.

Preparation of [{*cis*-Pt(NH$_3$)$_2$(9EtG-*N7*)}$_2$(μ-1,2,3-ta-*N1,N3*)](NO$_3$)$_3$ (5). A 20 mL sample of a water solution containing 0.133 g of [{*cis*-Pt(NH$_3$)$_2$}$_2$(μ-OH)(μ-1,2,3-ta-*N1,N2*)](NO$_3$)$_2$ (**2**) (0.2 mmol) and 0.0895 g of 9EtG (0.5 mmol) was stirred and incubated at 50 °C in the dark. During the incubation, the pH of the solution was kept at ca. 5 by careful addition of 0.5 M nitric acid. After 5 days, the solution was filtered and concentrated by rotary evaporator to 30% of its original. The solution was poured on a Sephadex G-10 (Pharmacia) column (3∅ × 11 cm, solvent H$_2$O, flow rate 0.85 mL/min, detection UV (254 nm)) to be purified a few times and lyophilized. The recrystallization was carried out from water.

Yield: 0.078 g (35%). Anal. Calcd for $C_{16}H_{32}N_{20}O_{11}Pt_2\cdot 2H_2O$: C, 17.36; H, 3.28; N, 25.31. Found: C, 17.32; H, 3.26; N, 25.20.

Preparation of [{*cis*-Pt(NH$_3$)$_2$(9EtG-*N7*)}$_2$(μ-4-phe-1,2,3-ta-*N1,N3*)](NO$_3$)$_3$ (6). A 20 mL sample of a water solution containing 0.149 g of [{*cis*-Pt(NH$_3$)$_2$}$_2$(μ-OH)(μ-4-phe-1,2,3-ta-*N1,N2*)](NO$_3$)$_2$ (**3**) (0.2 mmol) and 0.0895 g of 9EtG (0.5 mmol) was stirred and incubated at 50 °C in the dark. During the incubation, the pH of the solution was kept at ca. 5 by careful addition of 0.5 M nitric acid. After 5 days, the solution was filtered and concentrated by rotary evaporator to 30% of its original. The solution was poured on a Sephadex G-10 (Pharmacia) column (3∅ × 1 cm, solvent H$_2$O, flow rate 0.85 mL/min, detection UV (254 nm)) to be purified a couple of times and lyophilized. The resulting powder was recrystallized from water.

Yield: 0.093 g (39%). Anal. Calcd for $C_{22}H_{36}N_{20}O_{11}Pt_2\cdot 2H_2O$: C, 22.33; H, 3.41; N, 23.69. Found: C, 22.23; H, 3.30; N, 23.38.

X-ray Structural Determination. Single crystals of **3** were obtained by slow evaporation of its saturated water solution. X-ray intensities were collected at 150(2) K on a Nonius KappaCCD diffractometer with rotating anode and graphite monochromator (Mo Kα radiation, λ = 0.71073 Å). The structure was solved by automated Patterson techniques (DIRDIF 97[22]) and refined on F^2 by full-matrix least-squares techniques

(13) Kraker, A. J.; Hoeschele, J. D.; Elliott, W. L.; Showalter, H. D. H.; Sercel, D.; N. P. Farrell, *J. Med. Chem.* **1992**, *35*, 4526.
(14) Farrell, N.; Qu, Y.; Bierbach, U.; Valsecchi, M.; Menta, E. In *30 years of Cisplatin, Chemistry and Biochemistry of a leading Anticancer Drug*; Lippert, B., Ed.; Verlag CH: Basel, Switzerland, 1999; p 479.
(15) Brabec, V.; Kasparkova, J.; Vrana, O.; Novakova, O.; Cox, J. W.; Qu, Y.; Farrell, N. *Biochemistry* **1999**, *38*, 6781.
(16) Komeda, S.; Ohishi, H.; Yamane, H.; Harikawa, M.; Sakaguchi, K.; Chikuma, M. *J. Chem. Soc., Dalton Trans.* **1999**, *17*, 2959.
(17) Komeda, S.; Lutz, M.; Spek, A. L.; Chikuma, M.; Reedijk, J. *Inorg. Chem.* **2000**, *19*, 4230.
(18) Kozelka, J.; Segal, E.; Bois, C. *J. Inorg. Biochem.* **1992**, *47*, 67 (26).
(19) Tanaka, Y.; Velen, S. R.; Miller, S. I. *Tetrahederon* **1973**, *29*, 3271.
(20) Faggiani, R.; Lippert, B.; Lock, C. J.; Rosenberg, B. *J. Am. Chem. Soc.* **1977**, *99*, 777.
(21) López, G.; Ruiz, J.; Garcia, G.; Vicente, C.; Rodríguez, V.; Sánchez, G.; Hermoso, J. A.; Martínez-Ripoll *J. Chem. Soc., Dalton Trans.* **1992**, *10*, 1681.

Table 1. Crystal data for [*cis*-{Pt(NH$_3$)$_2$}$_2$(μ-OH)(μ-4-phe-1,2,3-ta-*N1,N2*)](NO$_3$)$_2$ (**3**)

compd no.	**3**
chemical formula	$C_8H_{19}N_9O_7Pt_2$
formula weight	743.50
crystal system	orthorhombic
space group	$Pca2_1$ (no. 29)
a [Å]	12.6313(2)
b [Å]	20.5633(2)
c [Å]	7.0390(1)
V [Å^3]	1828.32(4)
Z	4
ρ_{calc} [g/cm^3]	2.701
μ [mm^{-1}]	15.34
abs. correction	analytical
transmission	0.20−0.72
crystal color	colorless
crystal size [mm^3]	0.02 × 0.05 × 0.11
no. of reflcns measd	49143
no. of unique reflcns	4178
no. param./restraints	266/142
$R1$(all reflcns)	0.0354
$R1$(obsd reflcns)	0.0340
w$R2$(all reflcns)	0.0932
w$R2$(obsd reflcns)	0.0921
resid. dens. [e Å^3]	−2.19/1.86

(SHELXL 97[23]). All structural drawings and geometrical calculations were performed with PLATON.[24] The discrimination between the geometrically equivalent, but chemically different atoms N3 and C5 was based on the refinement of occupation factors. The nitrate anions were severely disordered. Further details of the crystal structure determination are given in Table 1.

NMR Measurements. Regarding the characterization of complexes **3**−**6**, and the pH titration and temperature dependence experiment, NMR measurements were performed on a 300 MHz Bruker DPX300 spectrometer in D_2O at 298 K (295−325 K for the temperature dependence experiment). ^{1}H and ^{195}Pt NMR chemical shifts were referenced to TSP (sodium 3-trimethylsilylpropionate-*2,2,3,3-d*$_4$) and Na_2PtCl_6 ($\delta = 0$), respectively.

A 2D ^{1}H−^{1}H NOESY spectrum of **6** in D_2O (pD 6.5) was acquired on a Bruker DMX 600 MHz at 293 K with a mixing time of 500 ms, using the Watergate gradient pulse for minimization of the water signal.[25] Four hundred increments in t_1 were collected with 2048 complex data points in t_2, and 8 scans at a sweep width of 6000 Hz.

Reactions in the NMR Tube. Each reaction of **1**, **2**, and **3** (4mM) with stoichiometric amounts of 9EtG (8mM) was carried out in nonbuffer D_2O solution in the NMR tube. The solutions were maintained at 310 K in a water bath. ^{1}H NMR spectra were measured at different time intervals at 310 K and recorded on a Bruker DPX300 spectrometer. Due to the released OH^- from the platinum complexes, the pD for the reactions slightly increased during 10 days of the reactions (7.5 to 7.8, 7.8 to 8.2, and 7.7 to 8.2 for the reaction of **1**, **2**, and **3**, respectively).

Kinetic Analysis. The kinetic data obtained could be fit to second-order kinetics. Relative integration values of the 9-methyl group of 9EtG were used to determine the concentration of the reactants and final products as a function of time. For the determination of the second-order kinetic constants (k), the following equation was applied:

$$x/[2A_0(A_0 - x)] = kt \qquad (1)$$

where A_0 is the initial concentration of the reactant (**1**, **2**, and **3**) and x is the concentration of the final product (1:2 complex) at time t. The k values obtained correspond to the first steps of the series of the reactions (see Scheme 1).

pH-Titration Experiments. Solutions of **4**, **5**, and **6** (2.0 mM) were prepared in D_2O, and pD was adjusted by 0.1 M DNO_3 and NaOD and measured at 298 K using a PHM 80 pH meter (Radiometer) before and after each ^{1}H NMR measurement. The pH-titration data were analyzed by using the equation:

$$\delta = (\delta_A[H^+] + \delta_B K_a)/([H^+] + K_a) \qquad (2)$$

where K_a is the average acid dissociation constant of two N1H protons of 9EtG ligands in **4**−**6** and δ_A and δ_B are respectively the chemical shifts of the 9EtG and 9EtG ligands of **4**−**6**. For curve fitting, the program KaleidaGraph (Synergy Software, Reading, PA; courtesy of Dr. J. Kozelka (Paris)) was used. pK_{a/D_2O} values obtained in D_2O were transformed to H_2O solution pK_{a/H_2O}.[26]

Temperature-Dependent NMR Experiments. Solutions (1.0 mM) of **4** (pD 6.8), **5** (pD 6.7), and **6** (pD 6.5) were prepared in D_2O, and used for the ^{1}H NMR measurements at a certain range of temperature (295−325 K).

Cytotoxic Studies. (a) Cell and Culture Condition. The L1210 murine leukemia cell line (JCRB 9026) was obtained from Health Science Research Resources Bank (Osaka, Japan). The cisplatin-resistant L1210 (L1210(cisPt)) was obtained by exposure of L1210 to 10 μM cisplatin over a period of 3 months. L1210 and L1210-(cisPt) were cultured in suspension in RPMI 1640 medium (Sigma) supplemented with 10% heat-inactivated fetal calf serum and no antibiotics. The cells were grown at 37 °C in a 5% CO_2 humidified atmosphere.

(b) Cytotoxicity Assay. Cytotoxicity was determined by MTT assay.[27] In brief, 200 μL aliquots of a cell suspension containing 10^5 cells/mL were pipetted into each well of the 96-well microtiter plate. The cells were treated for 48 h in the presence of various concentrations of platinum complexes. Following exposure to the drugs, 10 μL of a 50 mg/mL MTT solution was added to each well and the plate was left at 37 °C for 4 h. Then the culture media were removed and the plate was washed with PBS. The precipitated dye was solubilized by adding 200 μL of 2-propanol. The absorbance was measured by using a microplate reader at 570 nm. The IC_{50} value was defined as the drug concentration that reduced the absorbance by 50% of drug free control.

Results and Discussion

Crystal Structure of [{*cis*-Pt(NH$_3$)$_2$}$_2$(μ-OH)(μ-4-phe-1,2,3-ta-*N1,N2*)](NO$_3$)$_2$ (3). Compound **3** crystallizes in the achiral space group $Pca2_1$ with $Z = 4$. Just as in the reported crystal structure of **2**,[17] both enantiomers are present in equal amounts. A molecular plot of the structure is depicted in Figure 2. Selected bond lengths and angles are given in Table 2. The coordination of the Pt atoms is square planar (angle sums 359.9 and 360.0°) with an interplanar angle of 11.4(5)° between the coordination planes resulting in a Pt1···Pt2 distance of 3.4436(5) Å. The Pt−N distances are in the expected range, with the Pt−N-(ammine) distances slightly longer (2.015(9)−2.044(8) Å) than the Pt−N(ta) distances (1.985(8)−1.996(8) Å). A weak intramolecular hydrogen bond is observed with N9 of an ammine ligand as donor and the noncoordinated N3 of the triazolate as acceptor, quite similar to that in the crystal structure of **2**.[17] The phenyl plane is tilted from the 1,2,3-ta plane by 17.5(6)°. In the lattice the flat molecules are stacked on each other in the

(22) Beurskens, P. T.; Admiraal, G.; Beurskens, G.; Bosman, W. P.; Garcia-Granda, S.; Gould, R. O.; Smits, J. M. M.; Smykalla, C. The DIRDIF97 program system, Technical Report of the crystallography Laboratory, University of Nijmegen, 1997.
(23) Sheldrick, G. M. SHELXL-97, Program for Crystal Structure Refinement, University of Göttingen, 1997.
(24) Spek, A. L. *PLATON−a multipurpose crystallographic tool*; Utrecht University, The Netherlands, 2001.
(25) Sklenar, V.; Piotto, M.; Leppik, R.; Saudek, V. *J. Magn. Reson.* **1993**, *102*, 241.
(26) Martin, R. B. *Science* **1963**, *139*, 1198.
(27) Mossmann, T. *J. Immunol. Methods* **1983**, *83*, 55.

Scheme 1. Supposed Reaction Schemes of **1**, **2,** and **3** with 2 Equiv of 9EtG in Aqueous Solution

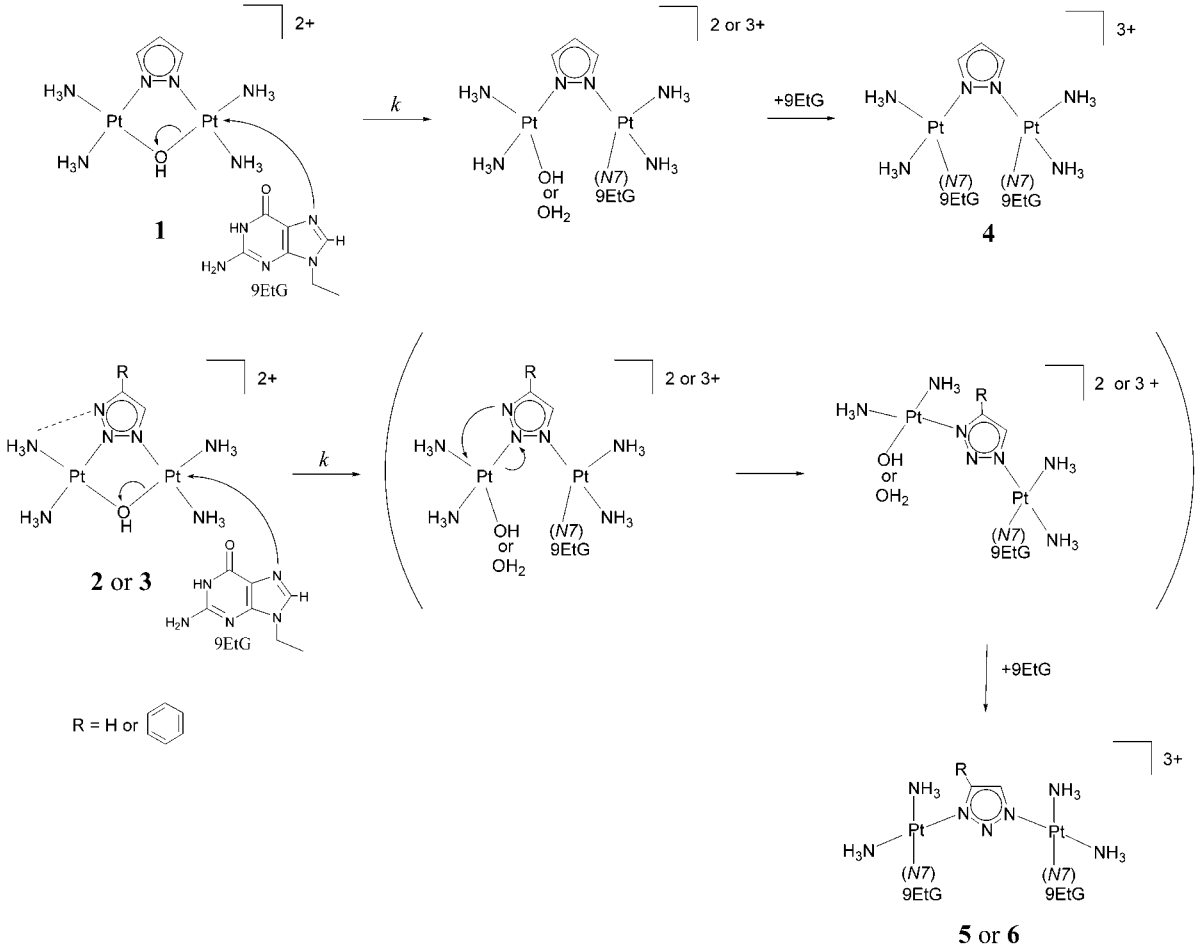

direction of the crystallographic *c*-axis. The Pt complex is involved in extensive intermolecular hydrogen bonding with the hydroxo and ammine groups as hydrogen bond donors and the oxygen atoms of the nitrates as acceptors.

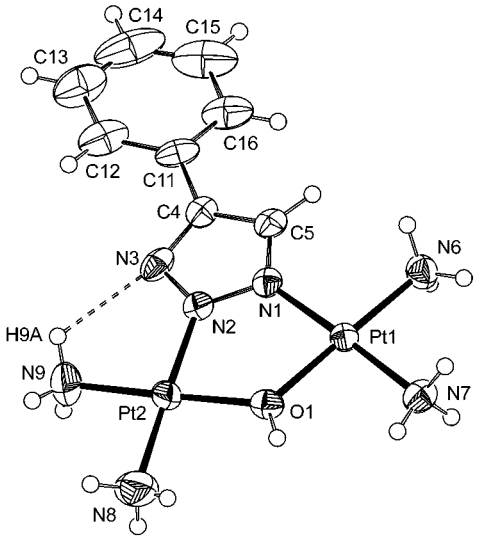

Figure 2. Displacement ellipsoid plot (50% probability) of the cation [{*cis*-$Pt(NH_3)_2$}$_2$(μ-OH)(μ-4-phe-1,2,3-ta-*N1,N2*)]$^{2+}$ (**3**) in the crystal structure. The nitrate anions were omitted for clarity. H-atoms were introduced at calculated positions and the ammine hydrogens were refined with a rotating model. The Dotted line indicates the formation of a hydrogen bond between the ammine ligand and the N3 of the 1,2,3-ta (N9···N3 2.911(16)Å, H9A···N3 2.37 Å, N9−H9A···N3 118°).

Table 2. Selected Bond Distances (Å) and Angles (deg) in [{*cis*-$Pt(NH_3)_2$}$_2$(μ-OH)(μ-4-phe-1,2,3-ta-*N1,N2*)]$(NO_3)_2$ (**3**)

Pt(1)−Pt(2)	3.4436(5)	Pt(2)−N(2)	1.984(8)
Pt(1)−N(1)	1.995(8)	Pt(2)−O(1)	2.028(7)
Pt(1)−O(1)	2.027(7)	Pt(2)−N(9)	2.025(11)
Pt(1)−N(6)	2.016(8)	Pt(2)−N(8)	2.036(11)
Pt(1)−N(7)	2.044(9)		
N(1)−Pt(1)−O(1)	89.3(3)	N(2)−Pt(2)−N(9)	89.7(5)
N(1)−Pt(1)−N(6)	91.2(3)	O(1)−Pt(2)−N(9)	178.7(4)
O(1)−Pt(1)−N(6)	179.2(3)	N(2)−Pt(2)−N(8)	178.0(5)
N(1)−Pt(1)−N(7)	177.7(3)	O(1)−Pt(2)−N(8)	89.7(5)
O(1)−Pt(1)−N(7)	88.4(3)	N(9)−Pt(2)−N(8)	91.1(6)
N(6)−Pt(1)−N(7)	91.1(4)	Pt(1)−O(1)−Pt(2)	116.2(3)
N(2)−Pt(2)−O(1)	89.5(3)		

Reaction of 1 with 9EtG. As some of us reported, complex **1** reacts with 2 equiv of 9EtG.[16] Incubating **1** with 2 equiv of 9EtG at 310 K, the pyrazole proton of **1** and the H8 and 9-ethyl signals of free nucleobase decrease in intensity, whereas the corresponding peaks assigned to the final product (1:2 complex), [{*cis*-$Pt(NH_3)_2$(9EtG-*N7*)}$_2$(μ-pz)]$^{3+}$ (**4**), appear and become larger (Figure 3, I). The supposed intermediate (1:1 complex) species could hardly be traced and identified at this reaction condition, clearly indicating that the rate-determing step is the substitution of a N7 in 9EtG for a OH bridge (see Scheme 1). The H8 signals in **4** are observed at higher field compared to that of free 9EtG, clearly due to the stacking interaction between intramolecular bases, which compensates for the inductive effect originating from platinum(II) coordination.[16,28] The pz protons are shifted to lower field, which is ascribed to the ring opening

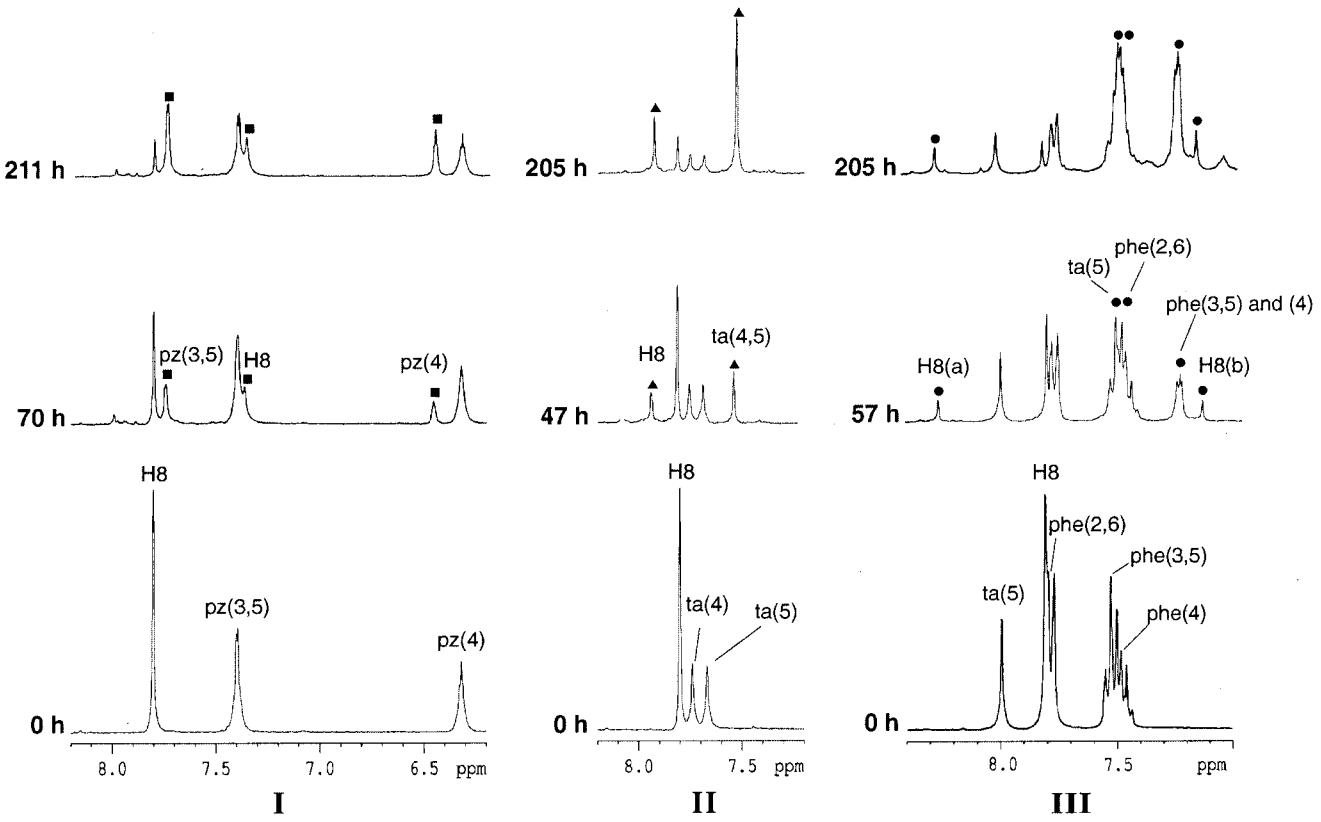

Figure 3. ^{1}H NMR spectra in the aromatic regions on the reactions of **1** (I), **2** (II) and **3** (III) with 2 equiv of 9EtG in D_2O measured at 310 K. The symbols show the H8 signals of 9EtG ligands, azole, and phenyl protons in the corresponding 1:2 complexes, [{*cis*-Pt(NH_3)$_2$(9EtG-*N7*)}$_2$(μ-pz)]$^{3+}$ (**4**; ■), [{*cis*-Pt(NH_3)$_2$(9EtG-*N7*)}$_2$(μ-1,2,3-ta-*N1,N3*)]$^{3+}$ (**5**; ▲), and [{*cis*-Pt(NH_3)$_2$(9EtG-*N7*)}$_2$(μ-4-phe-1,2,3-ta-*N1,N3*)]$^{3+}$ (**6**; ●), respectively. pD for the reactions slightly increased during the 9 days of reaction (7.5 to 7.8, 7.8 to 8.2, and 7.7 to 8.2 for the reactions of **1**, **2**, and **3**, respectively).

Table 3. The ^{1}H and ^{195}Pt NMR data (δ) and pK_{a/H_2O} values of N1H of 9EtG Ligands for [{*cis*-Pt(NH_3)$_2$(9EtG-*N7*)}$_2$(μ-pz)](NO_3)$_3$ (**4**), {*cis*-Pt(NH_3)$_2$(9EtG-*N7*)}$_2$(μ-1,2,3-ta-*N1,N3*)](NO_3)$_3$ (**5**), and [{*cis*-Pt(NH_3)$_2$(9EtG-*N7*)}$_2$(μ-4-phe-1,2,3-ta-*N1,N3*)](NO_3)$_3$ (**6**)[a]

	^{1}H					
	base					[a] pK_{a/H_2O} at
compd	H(8)	CH_2	CH_3	azole	^{195}Pt	N1H
4	7.47	3.84	1.22	7.87 (pz(3,5)) 6.55 (pz(4))	−2441	8.22 ± 0.04
5	8.13	4.12	1.41	7.51 (ta(4,5))	−2467	7.90 ± 0.01
6	8.35(a)	4.12(a)	1.40(a)	7.41 (ta(5))	−2466	7.94 ± 0.04(a)
	7.35(b)	3.80(b)	1.18(b)		−2476	7.86 ± 0.04(b)

[a] pK_{a/D_2O} values obtained in D_2O were transformed to H_2O solution (pK_{a/H_2O}).[25]

by the first substitution of N7 decreasing the electron population around the Pt-pz-Pt moiety.

Reaction of 2 with 9EtG. Complex **2** was also reacted with 9EtG in a bifunctional way, similar to **1**. Surprisingly, two interesting aspects different from **1** were observed on the reaction of **2**. One is that the H8 resonance assigned to the 1:2 complex appears at lower field (see Figure 3, II), as is commonly observed in metal-coordinated nucleobases, indicative of a weaker stacking interaction compared to product **4** obtained from **1**. The other is that the two independent proton signals of asymmetrically arranged 1,2,3-ta(4) and -(5) for **2** are observed at higher field as a single resonance for **5**. (Earlier[17] the ^{1}H NMR signals of ta(4) and ta(5) were not assigned correctly. The correct characterizations are 7.74 (ta(4)) and 7.67 (ta(5)), respectively.) In addition, the ^{195}Pt NMR signal for **5** appears as a single peak at −2467 ppm, i.e., in the range of PtN_4 chromophore,[29] while that of **2** was observed as two signals at −2101 and −2147 ppm.[17] This unusual behavior must indicate that the molecular configuration of **5**, contrary to **2**, possesses symmetry about the bridging 1,2,3-ta ring. From this observation it is clear that the reaction must involve a novel isomerization process, in which the Pt atom, initially bound to N2, migrates to N3 on the 1,2,3-ta ring, after the first substitution by N7 of 9EtG (see Scheme 1). In other words, after the first substitution accompanying the ring-opening, N3 substitutes for N2 to coordinate to the Pt atom. This isomerization reaction does not take place without guanine base under similar conditions (in D_2O, pD 5.6, 310 K) and is likely to be irreversible, as further migrations (i.e. N1 to N2) were not observed. Presuming the electron density concerning N2 and N3 before the migration, N2 must be less basic because more directly it experiences an inductive effect from the N1-coordinated platinum(II). Moreover, the first 9EtG substitution will result in rotation about the Pt2−N2 axis, which has the hydrogen bond (ammine-N3) broken. After this process N3 will increase its nucleophilicity. The higher field shift of the 1,2,3-ta protons (ta(4) and ta(5)) agrees with this. So the presence of platinum atoms at N1 and N3 results in decreased electron negativity of these nitrogen atoms, compared to the case of N1 and N2 platinum coordination, leading to less deshielded circumstances around C4 and C5. In addition, comparing the intramolecular Pt···Pt distance

(28) Odani, A.; Shimata, A.; Masuda, H.; Yamauchi, O. *Inorg. Chem.* **1991**, *30*, 2133.

(29) O'Halloran, T. V.; Lippard, S. J. *Inorg. Chem.* **1989**, *28*, 1289.

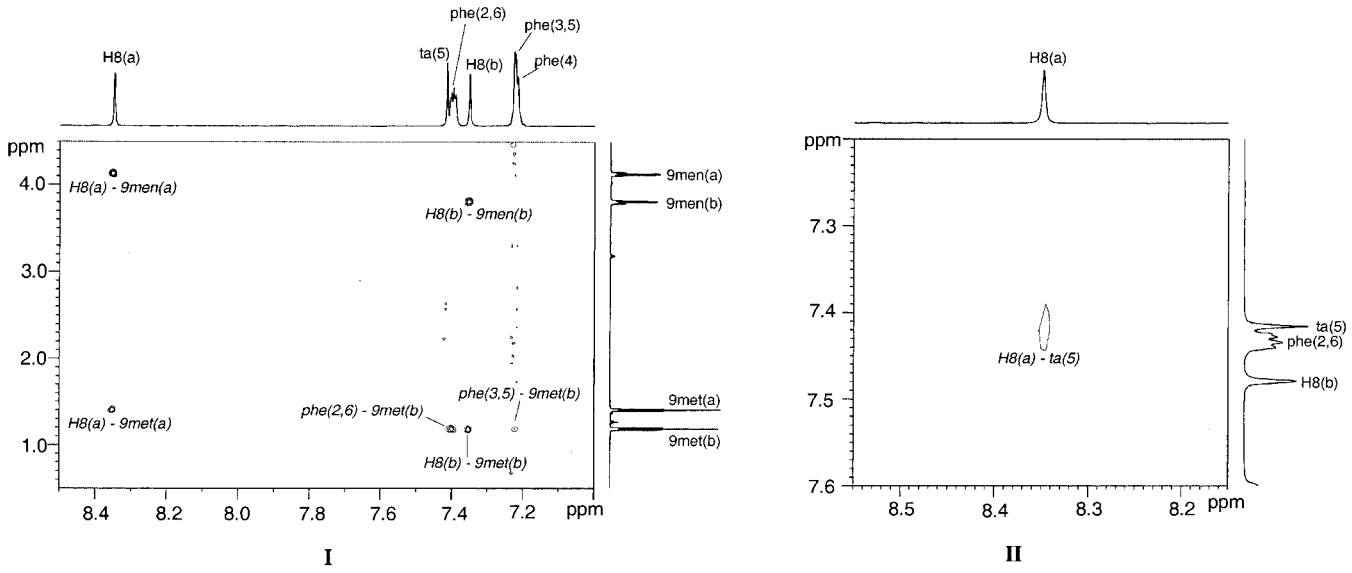

Figure 4. 2D ^{1}H−^{1}H NOESY spectrum of [{*cis*-Pt(NH$_3$)$_2$(9EtG-*N7*)}$_2$(*μ*-4-phe-1,2,3-ta-*N1,N3*)](NO$_3$)$_3$ (**6**) in D$_2$O (pD 6.5) at 293 K, showing the region of the cross-peaks between aromatic protons and 9-methylene (9men) and 9-methyl (9met) protons (I), and the cross-peak between H8(a) and ta(5) (II).

of the crystal structures of pz-bridged complex **1** and **4**, the distance of **4** is significantly (0.25 Å) longer than that of **1**.[16] This fact may indicate that N1 and N2 coordination on this type of 1:2 complex would be sterically constrained by a close proximity of the two guanine ligands.

Any intermediate species (see Scheme 1) could not be detected, showing that this migration takes place significantly faster than the first substitution reaction. It is not easy to find out which of the two reactions, i.e., the isomerization or the second 9EtG coordination, occurs first. The question of to which platinum atom the first guanine binds is also ambiguous. In the crystal structure of **2**, an intramolecular hydrogen bond is observed between the ammine ligand and N3 of the 1,2,3-ta ring.[17] Due to the formation of this hydrogen bond, the Pt2 coordination sphere might be thermodynamically more stable, and therefore, the first substitution might preferentially occur at the Pt1 coordination site.

Reaction of 3 with 9EtG. Complex **3** appears to react with 2 equiv of 9EtG to form a 1:2 complex with a small amount of intermediate species as well. While H8 of free 9EtG decreases in intensity, two new H8 signals appear simultaneously (see Figure 3, III). Interestingly, one H8 proton signal shows a lower field shift (H8(a)), whereas the other shifts to higher field (H8(b)). Both of these two signals, H8(a) and H8(b), increase in intensity as a function of time at the same rate and are likely to originate from two 9EtG ligands coordinated to the same molecule. **3** possesses a phenyl group at the C4 position of 1,2,3-ta as an electron-withdrawing substituent. Therefore, a decrease in nucleophilicity of the nitrogen atoms and steric hindrance around N3 would be expected to slow the N2−N3 migration of the Pt2 atom, as found in the reaction of **2**. However, the results obtained suggest that this isomerization also takes place immediately after the first substitution by N7 of 9EtG, just as in case of the reaction of **2**. All the 1,2,3-ta and 4-phenyl protons of **6** are shifted to higher field, as in the case of **2**. The ^{195}Pt NMR signals of **3** were observed at −2098 and −2149 ppm. Species **6** gives two resolved ^{195}Pt NMR signals at −2466 and −2476 ppm, both of which are in the range of the PtN$_4$ chromophore,[29] showing the small difference of the two platinum atom environments. The difference originates from the asymmetrically arranged 1,2,3-ta from the presence of the 4-phenyl substituent on 1,2,3-ta.

To further characterize **6**, a 2D ^{1}H−^{1}H NOESY experiment was performed. The region of the cross-peaks between aromatic protons and CH$_2$(9) and CH$_3$(9) in **6** is drawn in Figure 4, I. The intraresidual NOE cross-peaks were observed between the H8 and the 9-ethyl protons (H8(a)−9met(a)), H8(a)−9men(a), H8(b)−9met(b), and H8(b)−9men(b)). An interesting aspect is that only for the 9EtG(b) ligand were interresidual NOE cross-peaks observed between its 9-methyl protons (9met(b)) and some of the phenyl protons (phe(2,6) and phe(3,5)). This result clearly indicates that the platinum atom migration from N2 to N3 has brought the 9EtG(b) ligand in close proximity to the 4-phenyl group, resulting in higher field shift of H8(b), CH$_3$(9), and CH$_2$(9) by the ring-currency effect of the phenyl group. On the other hand, for the 9EtG(a) ligand, no cross-peak was observed with any phenyl proton, but instead with the ta(5) proton (H8(a)−ta(5)) (see Figure 3, -II). Thus, the lower field shift of H8(a) can be simply ascribed to the inductive effect by platinum coordination at N7.

pH Dependence on Chemical Shift and Half-Width of the H8 Signals in 4−6. Further details on the migration reaction have been deduced from the characteristics of the H8 proton resonances. Therefore, pH-titration experiments were performed on the H8 protons of **4**−**6** in D$_2$O (see Figure 5, I). For the 9EtG ligands in all complexes, the absence of N7 (de)-protonation in the acidic area is clear evidence for platinum coordination at N7. It is known that N7 coordination on guanine bases by platinum and some other transition metal cations acidifies the N1H site due to their electron-withdrawing effect.[30] A pH titration on a free 9EtG (0.4 mM, I = 0.1 M, 298 K) was performed, and the pK_{a/H_2O} of the N1H site derived from the titration curve is 9.73, in agreement with a previously reported value.[30] The corresponding pK_{a/H_2O} values for the N7-platinated 9EtG ligands in **4**−**6** were, as expected, found to be lower than those for free base. Hence, the pK_{a/H_2O} values obtained for **4**−**6**

(30) Song, B.; Zhao, J.; Griesser, R.; Meiser, C.; Siegel, H.; Lippert, B. *Chem. Eur. J.* **1999**, *5*, 2374.

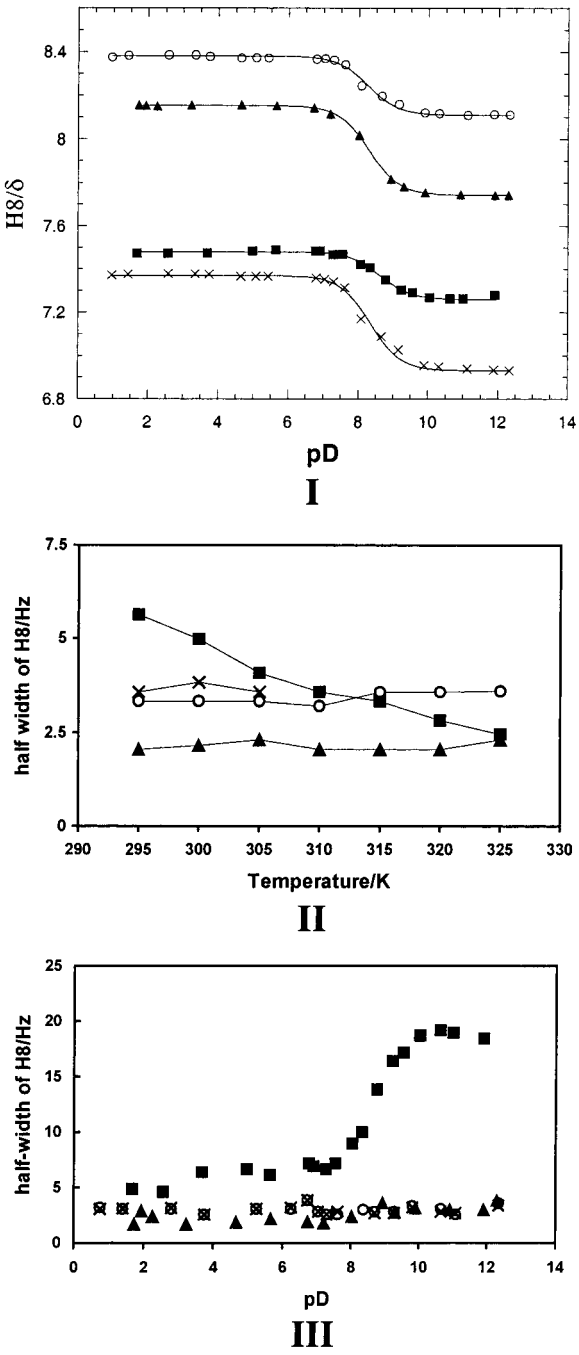

Figure 5. Plots of chemical shift (δ) of H8 resonance vs pD (**I**) of half-width (Hz) of H8 vs temperature (K) (II) and of half-width (Hz) of H8 vs pD (III) for [{*cis*-Pt(NH_3)$_2$(9EtG-*N7*)}$_2$(μ-pz)]$^{3+}$ (**4**; ■), [{*cis*-Pt(NH_3)$_2$(9EtG-*N7*)}$_2$(μ-1,2,3-ta-*N1,N3*)]$^{3+}$ (**5**; ▲), and [{*cis*-Pt(NH_3)$_2$(9EtG-*N7*)}$_2$(μ-4-phe-1,2,3-ta-*N1,N3*)]$^{3+}$ (**6**; H8(a), ○; H8(b), ×). pH-titrations were performed in nonbuffer aqueous solution at 298 K with adjusting pD with 0.1 N DNO_3 and 0.1 N NaOD. For H8(b) of **6**, exact half-width values were not measured at higher temperature (>305 K), due to the overlapping with phenyl proton peaks.

are listed in Table 3. The pK_a for **4** was found to be slightly larger than those for **5** and **6**, probably due to the increased basicity at the N1H site by a ring-currency effect resulting from the intramolecular stacking.

The plots of the half-width of the H8 resonance vs pD are redrawn in Figure 5, II. The half-width values for **4** are found to be significantly larger than that for **5** and those for **6** in this pD range. For instance, the half-width value of the H8 resonance of **4** was found to be 7.27 Hz (pD 6.66 at), and the others are 1.79 Hz (for **5**, pD 7.20) and 2.82 Hz (for both H8(a) and H8(b) in **6**, pD, 7.04) at 298 K. This implies that for **4** the intramolecular base−base stacking and hydrogen bonds must hinder the rotation about Pt−N7 (9EtG) axes,[31] and that the corresponding axes of **5** and **6** are likely to be relatively flexible (see Figure 6). Slow rotation of 9EtG about the Pt−N7 bond must be responsible for this broadening. To validate the correlation between axis flexibility, half-width values of the H8 signals were investigated as a function of temperature (see Figure 5, II). Exact half-width values for H8(b) of **6** were not measured at higher temperature (>305 K), due to the overlapping with phenyl proton peaks. As the temperature increases, the half-width of the H8 signal for **4** becomes smaller, reflecting the increased flexibility of the Pt−N7 axes. On the other hand, those for **5** and **6** seem to have no correlation with the solution temperature.

An aspect that should be emphasized is that for **4** the half-width increase occurs while the N1H experiences deprotonation, and that the behavior of the plot has a good correlation with the H8 chemical shift vs pD (see Figure 5, I and III). Accordingly, the most plausible explanation is that N1 deprotonation increases the ring-currency effect on the guanine bases, to provide more electron density to one another, resulting in further hindered rotation and loss of the flexibility about these Pt−N7 bonds in **4**. In addition, for the same reason, hydrogen bonds, supposedly formed more tightly between the ammine ligands and the O6 of guanines, may also contribute to such hindered rotation. For **5** and **6**, on the other hand, no correlation of the half-width value with respect to pD seems to be present, supporting the idea that the migration of the platinum from N2 to N3 provides unrestricted rotation around the corresponding axes owing to the more favorable arrangement of intramolecular guanine bases in the distance.

Kinetic Aspects. Hydrolysis is known to be the rate-limiting step for cisplatin ($t_{1/2} \sim 2$ h at 310 K),[32] which can be analyzed by first-order kinetics. In the reactions of these dinuclear complexes with 9EtG, the obtained kinetic data fit to second-order kinetics (see Figure 7). The presence of intermediate 1:1 complexes could hardly be traced and identified for the reactions of **1**−**3**. This absence confirms that the second N7 coordination, defined as a first-order reaction, takes place immediately after the first substitution. The second-order rate constants (k) for the first substitution step by N7 and half-life values ($t_{1/2}$) of free 9EtG for the reactions of **1**−**3** are listed in Table 4.

The first substitution of both triazole-bridged complexes (**2** and **3**) appears to proceed 1.6 times as fast as that of the pyrazole-bridged complex (**1**). Such a kinetic difference might be explained from the existence/absence of the intramolecular hydrogen bond between the ammine ligand and the azole. Accordingly, the formation of the hydrogen bond between the ammine ligand and N3(ta) in **2** and **3** would make the OH bridge less stable to promote the first substitution of 9EtG. **2** and **3** were found to react with 9EtG at almost the same rate, probably because the 4-phenyl group, the substituent on 1,2,3-ta of **3**, is located distant from the platinum coordination sphere (Pt1−C11, 5.566(10) Å; Pt2−C11, 5.433(11) Å). Therefore, the

(31) Bloemink, M. J.; Pérez, J. M. J.; Heetebrij, R. J.; Reedijk, J. *Inorg. Chem.* **1999**, *4*, 554.
(32) Bancroft, D. P.; Lepre, C. A.; Lippard, S. J. *J. Am. Chem. Soc.* **1990**, *112*, 6860.

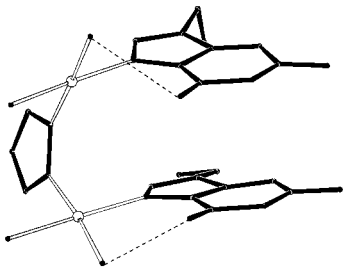

4

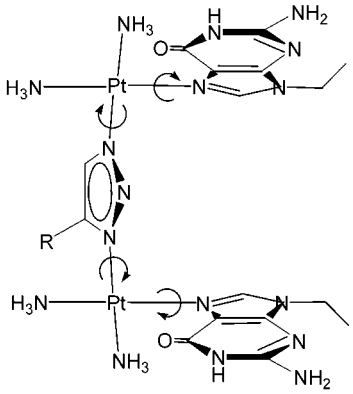

5 and **6**

Figure 6. Schematic representation of the crystal structure of **4**[16] and supposed structure of **5** and **6**. The dotted lines of **4** indicate the formations of hydrogen bonds between the ammine ligands and the O6 of the 9EtG ligands. Pt−N axes of **5** and **6** seem to be relatively flexible.

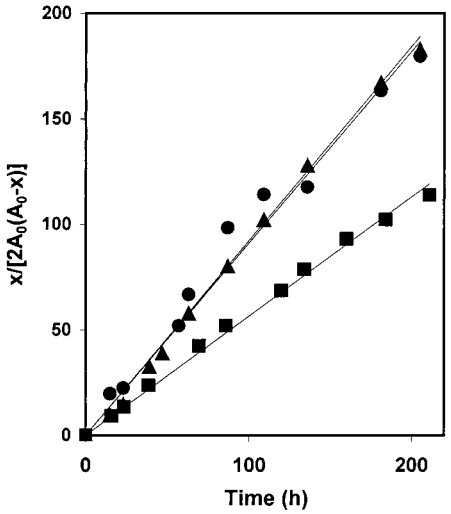

Figure 7. Second-order Guggenheim plots of the reactions of [{*cis*-Pt(NH$_3$)$_2$}$_2$(μ-OH)(μ-pz)]$^{2+}$ (**1**; ■), [{*cis*-Pt(NH$_3$)$_2$}$_2$(μ-OH)(μ-1,2,3-ta-*N1,N2*)]$^{2+}$ (**2**; ▲), and [{*cis*-Pt(NH$_3$)$_2$}(μ-OH)(μ-4-phe-1,2,3-ta-*N1,N2*)]$^{2+}$ (**3**; ●) with 9EtG in D$_2$O at 310 K. Values for *k* were calculated from the slope of the lines.

Table 4. Obtained Half-Life values ($t_{1/2}$ in h) and Second-Order Rate Constants (*k* in M^{-1} s^{-1}) for the Reactions of [{*cis*-Pt(NH$_3$)$_2$}$_2$(μ-OH)(μ-pz)]$^{2+}$ (**1**), [{*cis*-Pt(NH$_3$)$_2$}$_2$(μ-OH)(μ-1,2,3-ta-*N1,N2*)]$^{2+}$ (**2**), and [{*cis*-Pt(NH$_3$)$_2$}$_2$(μ-OH)(μ-4-phe-1,2,3-ta-*N1,N2*)]$^{2+}$ (**3**) with 2 Equiv of 9EtG in D$_2$O at 310 K

reaction	$t_{1/2}$ (h)	*k* (M^{-1} s^{-1})
1	221	1.57×10^{-4}
2	137	2.53×10^{-4}
3	135	2.56×10^{-4}

additional phenyl group is likely to have no major effect on the kinetics, resulting in marginal kinetic difference between **2** and **3**. Besides, forming the five-coordinated platinum(II) species with N7 at the axial position on the first substitution, the O6 of 9EtG will stay away from the π-electron-rich azolate group of **1**−**3**, due to the steric repulsion and to the hydrogen bondings with OH or ammine ligands. Consequently, quite less contact between 9EtG and the phenyl group can be anticipated. As proved above, it is clear that the reactions of **2** and **3** involve the isomerization after the first substitution. It is not clear which of these migrations on **2** or **3** proceeds faster, because of the difficulty in detecting the corresponding 1:1 and 1:2 complexes before the isomerization. However, judging from the expected basicity and steric hindrance, the isomerization on **2** might take place more rapidly than that on **3**.

Table 5. In Vitro Cytotoxicity Assay of the Dinuclear Platinum(II) Complexes, **1**−**3**, and Cisplatin on L1210 Murine Leukemia Cell Lines Sensitive (L1210(0)) and Resistant (L1210(cisPt)) to Cisplatin

	IC$_{50}$ (μM)		
test compd	L1210(0)	L1210(cisPt)	RF[a]
1	10.7 ± 1.1	15.0 ± 1.0	1.4
2	0.5 ± 0.2	1.1 ± 0.3	2.2
3	2.0 ± 0.2	11.6 ± 1.0	5.8
cisplatin	4.8 ± 0.3	19.3 ± 1.2	4.0

[a] Resistance factor (RF) is defined as the relative ratio of IC$_{50}$ values in both cell lines (L1210(cisPt)/L1210(0)).

Cytotoxic Studies. The cytotoxicity of complex **1**−**3** and cisplatin for comparison on L1210 murine leukemia cell lines sensitive and resistant to cisplatin is summarized in Table 5. In the parent cell line, **2** and **3** have exhibited higher cytotoxicity compared to cisplatin, especially, **2** is 10 times as active as cisplatin. **1** was found to be less cytotoxic than cisplatin, but still in the active range. The cytotoxicity of **1**−**3** in the resistant cell line exceeds that of cisplatin. Interestingly, **1** and **2** overcame cross-resistance to cisplatin, as expressed by resistance factors (RF = the relative ratio of IC$_{50}$ values in both cell lines (L1210-(cisPt)/L1210(0)) which are 1.4 and 2.2, respectively (4.0 for cisplatin). It is noteworthy that **2** was found to be 18 times more active than cisplatin in the resistant cell line.

Conclusions

The results presented above have unambiguously shown that platinum(II) atoms can migrate from N2 to N3 on the 1,2,3-ta rings through the reaction of **2** and **3** with 9EtG, and this isomerization is irreversible. It was recently reported that for cisplatin, bis(9-methyladenine) complexes of *cis*-Pt(II)(NH$_3$)$_2$ may undergo slow linkage isomerization, from N7 to N1, or to N6 on the adenine base in aqueous solution at elevated temperatures with concomitant loss of a proton (353−358 K).[33,34] In the present case this isomerization is not on the nucleobase, but instead a part of the platinum complex itself undergoes isomerization. The resulting widely opened platinum coordination sphere will expand a variety of possible cross-

(33) Arpalahti, J.; Klika, K. D.; Molander, S. *Eur. J. Inorg. Chem.* **2000**, *5*, 1007.
(34) Arpalahti, J.; Klika, K. D. *Eur. J. Inorg. Chem.* **1999**, *8*, 1199.

links on DNA. For instance, it can be expected that **2** and **3** can more readily form interstrand cross-links on double-strand DNA, compared to **1**. In addition, the other probable binding modes to DNA such as 1,3- and 1,4-intrastrand cross-links will also have to be anticipated. The local conformation of 1,2-intrastrand cross-links made by the pz-bridged complex and the 1,2,3-ta-bridged complexes might be distinct from each other. So, it will be of great interest to know whether the platinum(II) migration in **2** and **3** occurs on the d(GpG) site in larger oligonucleotides and DNA.

Judging from the kinetic properties, these azole-bridged dinuclear platinum(II) complexes are likely to react with DNA much slower than cisplatin and other derivatives that possess halide ions as leaving groups. Carboplatin has slightly stronger coordinating leaving group ligands, i.e., bis(carboxylato), than cisplatin, which makes the compound relatively less reactive.[35] This decrease in reactivity would account for the reduction of the side effects. Therefore, the slow kinetics may result in lower side effects, once these compounds are tested as drugs.

As our previously performed cytotoxic studies, **1** and **2** have shown remarkably higher activity than cisplatin in several human tumor cell lines,[17] and **3** has exhibited comparable cytotoxicity to cisplatin in a few of the cell lines (unpublished data). The current cytotoxicity assay has shown that **1** and **2** are effective against the L1210 cisplatin-resistant cell line and equally good as cisplatin on the parent cell line. The largely overcome cross-resistance might be ascribed to the sterically distinct adduct formation, i.e., the 1,2-intrastrand cross-link with minimal distortion, from cisplatin on inducing cytotoxic effects. Especially, **2** and **3** will be capable of providing several types of such different cross-links with latent isomerization ability.

Acknowledgment. The author is indebted to The Kidani Memorial Trust for a fellowship. Also travel support and sponsorship by COST Action D20/0001/00 (biocoordination chemistry) is kindly acknowledged. The authors are grateful to Johnson & Matthey (Reading, UK) for their generous loan of K_2PtCl_4. This research has been financially supported in part (M.L. and A.L.S.) by the Council for Chemical Science of The Netherlands Organization for Scientific Research (CW-NWO).

Supporting Information Available: Tables of crystal data, atomic coordinates, bond lengths and angles, anisotropic displacement parameters, hydrogen coordinates, and torsion angles (PDF). This material is available free of charge via the Internet at http://pubs.acs.org.

JA0168559

(35) Frey, U.; Ranford, J. D.; Sadler P. J. *Inorg. Chem.* **1993**, *32*, 1333.